# Soft Matter

## Accepted Manuscript

This article can be cited before page numbers have been issued, to do this please use: E. A. Crespo, L. F. Vega, G. Perez-Sanchez and J. A. P. Coutinho, *Soft Matter*, 2021, DOI: 10.1039/D1SM00362C.




ROYAL SOCIETY OF CHEMISTRY

rsc.li/soft-matter-journal

View Article Online
DOI: 10.1039/D1SM00362C

# Unveiling the Phase Behavior of $C_iE_j$ non-ionic surfactants in water through Coarse-Grain Molecular Dynamics Simulations

Emanuel A. Crespo,[a] Lourdes F. Vega,[b] German Perez-Sanchez,[a*,] and João A. P. Coutinho[a]

[a]CICECO – Aveiro Institute of Materials, Department of Chemistry, University of Aveiro, 3810-1933 - Aveiro, Portugal.

[b]Chemical Engineering Department and Research and Innovation Center on $CO_2$ and $H_2$ (RICH Center), Khalifa University of Science and Technology, P.O. Box 127788, Abu Dhabi, United Arab Emirates

[*]Corresponding author: gperez@ua.pt

View Article Online
DOI: 10.1039/D1SM00362C



## Abstract

Poly(oxyethylene) alkyl ethers, usually denoted by $C_iE_j$ surfactants, exhibit a rich phase behavior in water, self-assembling to form a variety of 3-D structures with a controllable morphology that find multiple applications, across different industrial segments. Hence, being able to describe and understand the effect of molecular structure on the phase behavior of these systems is highly relevant for the efficient design of new materials and their applications.

Considering the promising results obtained over the last decade using the MARTINI model to describe ethylene-oxide containing compounds, an extensive assessment of the ability of such model to describe the phase behavior of $C_iE_j$ in water was carried out and results are presented here. Given the overall poor temperature transferability of the MARTINI model, mostly due to the lack of an accurate representation of hydrogen bonding, simulations were carried at a single temperature of 333 K, where most phases are expected to occur according to experiments. Different chain lengths of both the hydrophobic and hydrophilic moieties, spanning a wide range of hydrophilic-lipophilic balance values, were investigated and the phase diagrams of various $C_iE_j$ explored in a wide concentration range. The model was able to satisfactorily describe the effect of surfactant structure and concentration on the mesophase formation. The stability and dimensions of the obtained phases, including the prediction of some unique features such as the characterization of a singular lamellar phase is presented. Results obtained in this work highlight both the predictive ability and the transferability of the MARTINI forcefield in the description of such systems. Moreover, the model was shown to provide adequate descriptions of the micellar phase in terms of micelle dimensions, critical micellar concentration, and average aggregation numbers.

**Keywords:** non-ionic surfactants, modelling CiEj mesophases, MARTINI forcefield, CiEj micelles

View Article Online
DOI: 10.1039/D1SM00362C



## 1. Introduction

Non-ionic surfactants such as poly(oxyethylene) alkyl ethers have a wide number of applications, across different industrial segments. From detergents and cosmetics to enhanced oil recovery, many other applications such as drug delivery, emulsification, proteins purification and crystallization, and others in the agriculture, textile, and paper industries have been reported.[1–3] Most of their success is due to their ability to, once in aqueous solution, self-assemble to form a variety of 3-D structures with a controllable morphology, ranging from simple spherical, rod, disk or worm-like micelles at low surfactant concentrations, to the formation of more complex liquid crystalline (LC) phases (e.g. hexagonal ($H_1$) or lamellar ($L_\alpha$) phases) at higher concentrations.[4]

Among the different non-ionic surfactants, linear poly(oxyethylene) alkyl ethers, whose general chemical formula is $H(CH_2)_i(OCH_2CH_2)_jOH$, often simply denoted by $C_iE_j$ surfactants, – $i$ represents the number of carbon atoms in the hydrophobic tail of the surfactant and $j$ the number of ethylene oxide (EO) groups – are particularly relevant. $C_iE_j$ surfactants are often known as reference detergents, and as archetypal systems to study fundamental aspects of non-ionic surfactant solutions. Owing to their simple molecular architecture, they are easy to synthesize (several $C_iE_j$ grades are commercially available), and their properties can be tuned, aiming at a specific application, by manipulating the length of the hydrophobic tail and hydrophilic moiety of the molecule.[5] As an example, the shapes and sizes of the self-assembled structures of systems containing $C_iE_j$ surfactants are useful as templates in the development of new materials, such as nano-porous structures with dimension-controlled pores.[6]

Therefore, understanding and ultimately predicting the role of the surfactants molecular structure on the properties of their aqueous micellar solutions, and on the morphology of the self-assembled structures, is highly relevant for the design and synthesis of new compounds and materials of interest for many applications.[7] On the other side, for some aspects of industrial handling, processing and transportation, it is important to avoid the formation of LC phases that exhibit marked gel-like properties, with considerable high viscosities hampering the preparation of useful formulations.[8]

Given the importance of these surfactants, both from a fundamental and a practical point of view, several experimental techniques were employed to characterize their rich phase behavior in

View Article Online
DOI: 10.1039/D1SM00362C



water, providing useful information both in the micellar regime,[9,10] and at higher amphiphile concentrations, where techniques like small-angle X-ray scattering (SAXS), small-angle neutron scattering (SANS), and polarizing optical microscopy (POM), among others, allow to investigate the formation of different LC phases and display their phase diagrams.[11,12] Unfortunately, an unequivocal identification of the mesophase formed under certain thermodynamic conditions and its microscopic structure is not an easy task, being the origin of conflicting results, especially when different experimental techniques are used. As an example, the phase diagram of $C_{10}E_5$/water reported by Nibu and Inoue[13] describes the existence of a bi-continuous cubic phase ($V_1$) in the composition range between the $L_\alpha$ and $H_1$ phases, while in the study of Lang and Morgan,[14] only the $L_\alpha$ and $H_1$ phases were reported; similar issues were also reported for other surfactants such as $C_{10}E_6$,[13,15,16] $C_{12}E_2$,[17,18] $C_{12}E_6$,[11,19] $C_{12}E_8$.[11,20–22]

By establishing a link between molecular structure and the fluids microscopic behavior, molecular dynamics (MD) simulations can be used to enhance our ability to identify the various phases observed experimentally and discern the most stable ones. Furthermore, MD simulations provide useful insights into the mechanisms ruling micellization, clouding or self-assembly phenomena. All-atom (AA) models, although being able to provide detailed and precise information about the initial stages of micelle formation in diluted systems,[3,7,23–26] are unable to address the time and size scales relevant for the self-assembling and mesophase transition processes. In this regard, the required relaxation times, typically in the order of microseconds at the nanometer scale, leave the AA models out of the way unless preformed structures are used. Conversely, coarse-grain (CG) models, constructed by grouping a certain number of atoms into a single interaction site, significantly reduce the computational demand, being a powerful tool to investigate the surfactant self-assembly and, consequently, to investigate the mesophase behavior of $C_iE_j$ surfactants in water.

Shinoda and co-workers[27] were the first to propose a coarse-grain model for the $C_iE_j$ surfactants. In their work, the intramolecular potentials were fitted to reproduce the bond and angle distributions obtained from more detailed AA-MD simulations, while the intermolecular interactions were fitted using density, surface tension and hydration free energy experimental data. However, for the interaction between the EO groups and water, since hydration free energy data was not available, they used structural data of the $L_\alpha$ phase in the $C_{12}E_2$/water system (e.g. lamellar spacing and molecular area) to parameterize this interaction, and showed that the model

View Article Online
DOI: 10.1039/D1SM00362C



was able to correctly describe such phase. Only on a later study carried out by the same authors,[28] the transferability and versatility of the model was assessed by extending the model to the $C_{12}E_6$ surfactant. The model predicted the existence of the micellar, $H_1$ (although thin water channels were found to persist between the cylinders) , and $L_\alpha$ phases at 20, 50 and 80 %wt of surfactant concentration, respectively, in agreement with experimental reports.[11,19]

However, the majority of the CG modelling of $C_iE_j$ surfactants in water[1,29–32] relied on the MARTINI forcefield (FF). Although this model was initially aimed for biomolecular simulations of phospholipids, the MARTINI FF has been increasingly successfully applied for a variety of chemical systems.[33] The adoption of the MARTINI FF is mainly due to its remarkable transferability, since it proposes a general coarse-graining framework, where molecules are mapped from a few pre-defined bead types (with different polarities and hydrogen bonding capabilities), whose interaction LJ potentials are systematically parameterized to match densities, self-diffusion constants, and partitioning free-energies of representative building blocks.[34]

The MARTINI FF have thus been applied to investigate the critical micellar concentration (cmc) and aggregation number ($N_{agg}$) of $C_iE_j$ surfactants in water.[1] The micellar assemblies of $C_{12}E_5$ and the existence of a sphere-to-rod transition with increasing surfactant concentrations,[29,35] or the self-assembly of micellar, hexagonal and lamellar phases of $C_{12}E_j$ ($j$ = 2, 4, 6) surfactants were also tackled.[31] Despite some promising results, the models available exhibited a limited transferability to compounds with a large number of EO units and the existent MARTINI beads were shown to be too hydrophilic to accurately represent an EO group,[31,33] being inappropriate for simulations in non-polar media.

To overcome such limitations, and to increase the numerical stability of these models, Grunewald et al,[36] recently proposed a new MARTINI bead to represent EO groups, carrying a systematic parameterization to ensure its full compatibility with the whole MARTINI energy matrix of interactions. The new model was successfully applied to describe the densities of bulk PEO oligomers, long-range structural properties of different PEO chains, structural properties of lipid bilayers containing pegylated lipids, and the phase behavior of some $C_iE_j$ surfactants, paving the way to the simulation of more complex systems containing EO groups. However, as previously done in the work of Rossi et al.[31], the simulations of non-ionic surfactants in water were carried only for three specific concentration/chain length pairs, namely $C_{12}E_2$, $C_{12}E_4$, and $C_{12}E_6$, with a surfactant composition of 71.1, 53, and 50 % (w/w), respectively. Consequently,

View Article Online
DOI: 10.1039/D1SM00362C



before using this surfactant model for more complex studies, such as in multi-component systems (e.g., by adding an oil, a salt, or a co-solvent to the aqueous solution), it is vital to assess the performance of the above-mentioned model under a wide variety of conditions and $C_iE_j$ surfactants. Therefore, the main aim of this work is to extend the MARTINI model for a wide range of $C_iE_j$ surfactants by carrying a systematic assessment of its performance. The effect of chain length (of both the hydrophobic and hydrophilic moieties) and the surfactant concentration on the phase behavior of $C_iE_j$/water is presented, while spanning a wide range of hydrophilic-lipophilic balance (HLB) values.

## 2. Methodology

The MD simulations performed in this work were carried out using the GROMACS 2019 package,[37] integrating the equations of motion using the leap-frog algorithm with a time step of 20 fs. The potential energy in the $C_iE_j$ surfactant CG model proposed by Grunewald et al.[36] is obtained as a sum of the contributions due to bond stretching, angle bending (including the use of a "restricted bending" potential developed by Bulacu and co-workers[38] for improved stability when one of the angles approaches 180º), and dihedrals for bonded interactions and a Lennard-Jones (LJ) potential to describe the non-bonded interactions. Examples of topology (.itp) files for a surfactant molecule were provided together with the original publication of the EO bead in the work of Grunewald et al,[36] while a schematic representation of the CG mapping considered for the $C_{12}E_6$ surfactant is provided in **Figure S1** in the Supporting Information as an example of the surfactants studied in this work. The alkyl groups are described using a 4:1 mapping by the apolar $C_1$ bead proposed in the original MARTINI FF;[34] the EO groups are represented by the EO bead ($OCH_2CH_2$) recently proposed in the work of Grunewald et al,[36] and the terminal hydroxyl group is modelled using a small-type polar bead, SP2, from the original MARTINI FF.[34]

Non-bonded interactions were computed using a Verlet cut-off scheme (Potential-shift-verlet modifier) with a cut-off length of 1.1 nm, changing the verlet-buffer-tolerance from its default value ($5 \cdot 10^{-3}$) to $10^{-5}$ kJ/mol/ps. The temperature of the simulation boxes was fixed using the velocity-rescaling thermostat,[39] with a coupling time constant, $\tau_T$ = 1.0 ps, while the pressure coupling was assured by the Parrinello-Rahman barostat[40] with a coupling time constant, $\tau_P$ =

View Article Online
DOI: 10.1039/D1SM00362C



24.0 ps. Before the production runs in the *NpT* ensemble, an equilibration procedure was followed for every simulation: an energy minimization step using the steepest descent method to prevent short-range contacts between atoms, followed by a short *NVT* run to ensure the right temperature of the simulation (5-10 ns) and a short simulation in the *NpT* ensemble to equilibrate the system density (20 ns). During the NVT equilibration step, the LINCS algorithm[41] was used to constrain the bond lengths to facilitate the equilibration of temperature in some of the more concentrated systems. For the production runs, the total energy profile of the systems was monitored, and the equilibrium assumed when the energy remained constant for at least 1 μs with an energy drift lower than 10 kJ/mol. A total simulation time of 6 μs was observed to be sufficient to ensure that all the investigated systems have reached their final equilibrium state. The equilibrium was also confirmed by monitoring temperature, pressure and density of the system as well as by visual inspection of the simulation boxes. To confirm that the simulations did not become trapped in a local minimum, as it may occur in CG simulations due to high energy barriers, the first 4 μs were carried out at the simulation temperature (333 K was used for all systems), followed by 1 μs at a higher temperature (363 K), and an additional 1 μs at the simulation temperature. This procedure was shown in a recent work with imidazolium-based ionic liquids (ILs) to help simulations reach their final equilibrium structure and overcome local minima.[42]

Every simulation was carried out using a cubic box with periodic boundary conditions (PBC) and an initial random configuration, generated using the PACKMOL code.[43] Simulations were visualized using the Visual Molecular Dynamics (VMD) software package,[44] and the micellar aggregates were analyzed using an in-house code[45] inspired by the Hoshen-Kopelman cluster-counting algorithm.[46] This algorithm considers that two surfactant molecules belong to the same aggregate when their tail sites are separated by less than a certain threshold, which is usually defined by the first minimum of the respective radial distribution functions. The aggregate sizes can then be monitored along the simulation trajectory, until reaching their final equilibrium value.

## 2.1. Simulated Systems

As mentioned in the introduction, the aim of this study is to extend the Grunewald et al.[36] model for a wide range of $C_iE_j$ surfactant aqueous solutions. This should allow to validate the

View Article Online
DOI: 10.1039/D1SM00362C



MARTINI FF for further studies of multicomponent systems containing such compounds. Therefore, twelve different surfactants, with various chain lengths of both the alkyl tail and hydrophilic moiety were selected to investigate the relationship between molecular structure and phase behavior. The simulated systems are reported in **Table 1** displaying a range of alkyl-chain lengths $i$ = 8, 12, and 16, while the number of EO units, $j$, varies between 2 and 23. The expression proposed by Griffin[47] to determine the hydrophilic-lipophilic balance (HLB) values was applied to the selected surfactants, as follows:

$$HLB = 20 * \frac{M_h}{M} \#(1)$$

where $M_h$ is the molar mass of the hydrophilic segment and $M$ is the molar mass of the surfactant molecule.

The values obtained from **equation 1** are displayed in **Table 1**. As can be gauged from **Table 1**, the selected surfactants span a wide range of HLB values (8.17-17.4), especially in the water-soluble region of the scale (values between 10-20 characterize water-soluble surfactants).

The overall $C_iE_j$/water systems were simulated at least at four different surfactant concentrations, namely 15, 30, 50, and 70 %wt. A few additional simulations at different concentrations were carried out for specific systems, whenever appropriate for further comparisons with experimental reports. Although there is a marked temperature effect on the phase diagram of $C_iE_j$/water systems (e.g. sphere to rod transitions, clouding phenomena, etc.), the MARTINI FF suffers from a poor temperature transferability, mainly due to the lack of an accurate representation of certain nonbonded interactions, such as hydrogen bonding. Consequently, changes in temperature are mainly advantageous to reduce the mixing entropy and to increase the kinetic energy, helping to avoid local minima during the calculations. Therefore, all the simulations were carried out at 333 K, a temperature slightly higher than most experimental observations.

**Table 1. Non-ionic surfactants studied in this work.**

| Surfactant | HLB | Experimental observations reported in Literature | Ref. | %wt of $C_iE_j$ in CG-MD simulations (%wt) | Phases observed in the simulations |
|---|---|---|---|---|---|
| $C_8E_6$ | 14.9 | $H_1$ | 11,16 | 15/30/50/60/70 | $L_1$, $H_1$ |
| $C_8E_{12}$ | 17.0 | No mesophases were observed. | 11 | 15/30/50/70 | $L_1$ |
| $C_{12}E_2$ | 8.17 | W, $L_3$, $L_2$, $V_2^{(1)}$, $V_2^{(2)}$, $L_\alpha$ | 17,18 | 15/30/45/50/70 | W, $L_3$*, $L_\alpha$ |
| $C_{12}E_4$ | 11.2 | W, $L_3$, $L_2$, $L_1$, $L_\alpha$ | 11 | 15/30/53/70/80 | $L_1$, $L_\alpha^H$, $L_\alpha$ |
| $C_{12}E_6$ | 13.0 | $H_1$, $L_\alpha$, $V_1$ | 11,19 | 15/30/50/70/80 | $L_1$, $H_1$, $V_1$, $L_\alpha^H$, $L_\alpha$ |
| $C_{12}E_{10}$ | 15.0 | $H_1$, $L_2$, $L_1$ | 48 | 15/30/50/70/85 | $L_1$, $H_1$ |
| $C_{12}E_{12}$ | 15.6 | Fm3m, Im3m, Pm3n, $H_1$ | 49 | 15/30/50/70/82 | $L_1$, $H_1$ |
| $C_{12}E_{23}$ | 17.4 | $L_1$, $I_1$, $L_2$ | 48 | 15/30/50/70 | $L_1$ |
| $C_{16}E_4$ | 9.62 | W, $L_2$, $L_3$, $V_2$, $L_\alpha$ | 11 | 15/30/50/70 | $L_1$, $V_1$, $L_\alpha$ |
| $C_{16}E_6$ | 11.5 | $N_c$, $L_1$, $L_\alpha^H$, $H_1$, $V_1$, Int, $L_\alpha$, $L_\beta$ | 50,51 | 15/30/40/50/70 | $L_1$, $H_1$, Int, $L_\alpha^H$, $L_\alpha$ |
| $C_{16}E_8$ | 12.8 | W, $L_1$, $I_1$, $H_1$, $V_1$, $L_\alpha$, $L_2$ | 11 | 15/30/50/70/80 | $L_1$, $I_1$*, $V_1$, $L_\alpha$ |
| $C_{16}E_{12}$ | 14.5 | W, $L_1$, $I_1$, $H_1$, $V_1$, $L_\alpha$ | 11 | 15/30/50/70/90 | $L_1$, $V_1$, $L_\alpha$ |

**Nomenclature:** $L_1$ – Micellar Solution; $L_2$ – Surfactant liquid; $L_3$ – 'critical' aqueous surfactant solution; $I_1$- cubic phase of close-packed micelles; $H_1$- normal Hexagonal phase; $V_1$ – normal bi-continuous cubic phase; Lα – Lamellar phase; $V_2$ – Reversed bi-continuous cubic phase; $V_2^{(1)}$ – bi-continuous cubic phase with Pn3m symmetry; $V_2^{(2)}$ – bi-continuous cubic phase with Ia3d symmetry; W – water containing surfactant unimer, usually continuous with $L_1$; Fm3m/Im3m/Pm3n – different arrangements of a micellar cubic phase; $N_c$- lyotropic nematic phase composed of rod-shaped micelles; $L_\alpha^H$ –lamellar phase with water-filled defects; $L_\beta$ – Gel phase; Int – non-cubic phases between $H_1$ and Lα occurring in $C_iE_j$/water systems when long alkyl chains prevent the formation of $V_1$.

* - the system is in a transition towards the indicated mesophase

View Article Online
DOI: 10.1039/D1SM00362C



## 3. Results and discussion

Aqueous solutions of $C_iE_j$ surfactants with short alkyl tails ($i < 8$) usually do not exhibit the formation of LC phases with a consequent mesophase instability for lower $i$ surfactants caused by the entropy increase associated with the formation of small micelles from rods or bilayers. Therefore, their phase diagrams usually feature only a two-phase liquid-liquid equilibrium (LLE) characterized by a lower critical solution temperature (LCST) and, in some cases, exhibiting a closed-loop type behavior with an upper critical solution temperature (UCST) emerging at higher temperatures. Examples of such phase diagrams were reported by Christensen and co-workers for both types of diagrams,[52] and are widely available in literature for a considerable number of surfactants.

The clouding phenomena leading to the phase separation is mainly driven by a temperature effect leading on long-range concentration fluctuations and a hypothetical micellar growth that are thought to be in the origin of the phase transition.[53,54] Unfortunately, as mentioned in the previous section, the CG models have a limited ability on capturing the effect of temperature. For this reason, the study of the macroscopic LLE of these surfactant solutions is, in our opinion, better tackled using other types of modelling techniques such as umbrella-sampling MD simulations, thermodynamic integration or the use of advanced molecular-based equations of state, derived from the Statistical Associating Fluid Theory.[55,56] Nevertheless, a complete description of the LLE equilibrium of $C_iE_j$/water systems is out of the purpose of this work. Instead, the simulations are focused on investigating the formation of the lyotropic LC phases observed for surfactants possessing higher alkyl chain lengths (typically $i >= 8$) as well as the impact of the surfactant molecular structure and concentration. The different phases observed in the CG-MD simulations are summarized in **Table 1** and will be discussed in the following sections, before concluding with some remarks on the more diluted micellar phase.

### 3.1. $C_8$ surfactants

The $C_8$ surfactant in water with two different EO groups, namely the $C_8E_6$ and $C_8E_{12,}$ were simulated. For the former, Clunie et al.[16] and Marland et al.[57] reported the existence of a $H_1$ phase in a narrow temperature range for surfactant concentrations between 50 and 70 %wt. The MD results for $C_8E_6$ at this concentration range are shown in **Figure 1**. At 50 %wt, the $C_8E_6$

View Article Online
DOI: 10.1039/D1SM00362C



system revealed the formation of cylindrical micelles resembling the hexagonal arrangement. Conversely, at 70 %wt concentration the $C_8E_6$ system displayed a transition state towards the formation of layers, in what should be the initial stage of the $L_\alpha$ phase that although not observed here, has been reported experimentally for $C_{10}E_6$.[14] Both concentrations were in reasonable agreement with the experimental reports since the 50 and 70 %wt concentrations are the lower and upper limits for the $H_1$ mesophase observed. An additional simulation at 60 %wt (the concentration at which such phase is, according to the literature, present in a wider temperature range) was carried out and the final equilibrium state is also shown in **Figure 1**. It clearly shows the hexagonal arrangement of the cylindrical micelles. The individual cylindrical micelles and their long-range organization can be clearly seen in **Figure S2** in the Supporting Information.

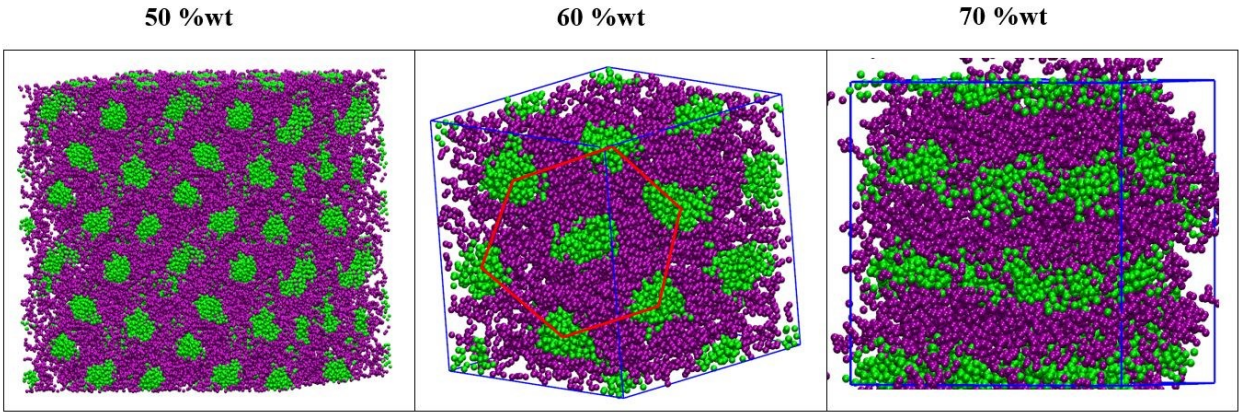


**Figure 1.** CG-MD simulations of $C_8E_6$ in water at different surfactant concentrations. Green represents the alkyl tail beads, while purple is used to represent the beads of the EO hydrophilic moiety. Water molecules are omitted for a clear visualization.

At lower concentrations, 15 %wt and 30 %wt, the MD $C_8E_6$ simulations were in good agreement with the literature reports.[16,57] As shown in **Figure S3** in Supporting Information, both concentrations consisted in a simple micellar solution with individual spherical or near-spherical micelles. Nonetheless, an increase in the size and elongation of the micelles was observed as the surfactant concentration increased, leading to a sphere-to-rod transition of the micelles being observed from 15 %wt to 30 %wt of surfactant.

For the $C_8E_{12}$ system, the increased number of EO units (higher HLB), exhibited a much higher affinity with water molecules that makes it much less prone to the formation of mesophases. Mitchell et al.[11] reported the absence of mesophases in aqueous solutions for $C_8E_4$,

View Article Online
DOI: 10.1039/D1SM00362C



$C_8E_8$, and $C_8E_{12}$. The CG-MD simulations were able to accurately predict the higher water affinity induced by the extra EO units, whose final snapshots are depicted in **Figure S4** in Supporting Information. **Figure S4** shows the existence of dispersed micelles of different sizes and shapes in the 15-50 %wt concentration range. Nonetheless, at 70 %wt, the simulation reveals the initial stages of formation of a $H_1$ – like phase that was not previously reported in the literature. This is the first time that the MARTINI FF is applied to $C_iE_j$ surfactants with $i \neq 12$ and it is in good agreement with the experiments, especially when predicting the mesophase instability of $C_8$ surfactants with a higher number of EO units, which can be interpreted as an indicator of the good transferability of the $C_iE_j$ CG model.

### 3.2. $C_{12}$ surfactants

It is widely accepted that, by increasing the alkyl chain length, the mesophase instability previously observed for $C_8$ surfactants is decreased, with the interactions between alkyl tails favoring the formation of LC phases even for those surfactants containing relatively short hydrophilic segments. To assess whether the MARTINI FF is able to capture such behavior, CG-MD simulations of six different $C_{12}$ surfactants with different EO groups in water were carried out, allowing to systematically study the effect of the number of EO units in the mesophase formation, spanning a wide range of HLB values (8.17-17.4).

At low HLB (lower number of EO units), Funari et al.[17] reported the phase diagram for the $C_{12}E_2$/water system. A striking feature of such phase diagram is the absence of an isotropic micellar phase in the low surfactant concentration regime, conversely to the majority of surfactant solutions. Instead, at 298 K, the micellar solution is replaced by a $L_\alpha$ phase – that is thought to coexist in equilibrium with water containing surfactant unimers. This $L_\alpha$ phase, present even at very low concentrations, is further found to persist up to approximately 80 %wt of surfactant concentration. The diagram proposed also suggests the formation of two reversed bi-continuous cubic phases with different morphologies ($V_2^{(1)}$ and $V_2^{(2)}$) and a sponge-like phase $L_3$ between 40-60 %wt in a narrow temperature range above the 303 K. A few years later, the same system was revisited by Lynch et al.[18] that proposed a new phase diagram for the same system. This new diagram essentially shares the same features described by Funari except for the presence of miscibility gaps between $L_3$/ $V_2^{(1)}$ and in between the two bi-continuous phases.

View Article Online
DOI: 10.1039/D1SM00362C



The CG-MD simulation results for the $C_{12}E_2$ system are shown in **Figure 2** where the $L_\alpha$ phase is indeed observed at low surfactant concentrations (15 %wt) persisting up to 70%wt, in excellent agreement with the experiments.[17,18] Literature CG-MD simulations have previously been carried out for this system but only at very high surfactant concentrations (around 70 %wt) for which the lamellar phase was also reported.[31,36] This is the first time that the formation of such phase in the low concentration regime, starting from random positions, is reported using CG-MD simulations. Unfortunately, no evidence for the formation of $L_3$ and $V_2$ phases was found in our simulations, what must be related to the narrow ($T$, $x$) experimental range in which they were observed. Accordingly to Funari et al.,[17] the interconversion between the $V_2$ phases is mainly driven by temperature rather than by surfactant concentration, thus being difficult to capture this phase in CG-MD simulations. Nonetheless, an additional simulation at 45 %wt was carried out at 303 K where Lynch and co-workers[18] reported the existence of an $L_3$ phase. The CG-MD result shown in **Figure 2**, points towards the formation of bended bilayers that can represent an intermediate stage towards the formation of a sponge-like phase, commonly suggested as a possible structure of the $L_3$ phase.

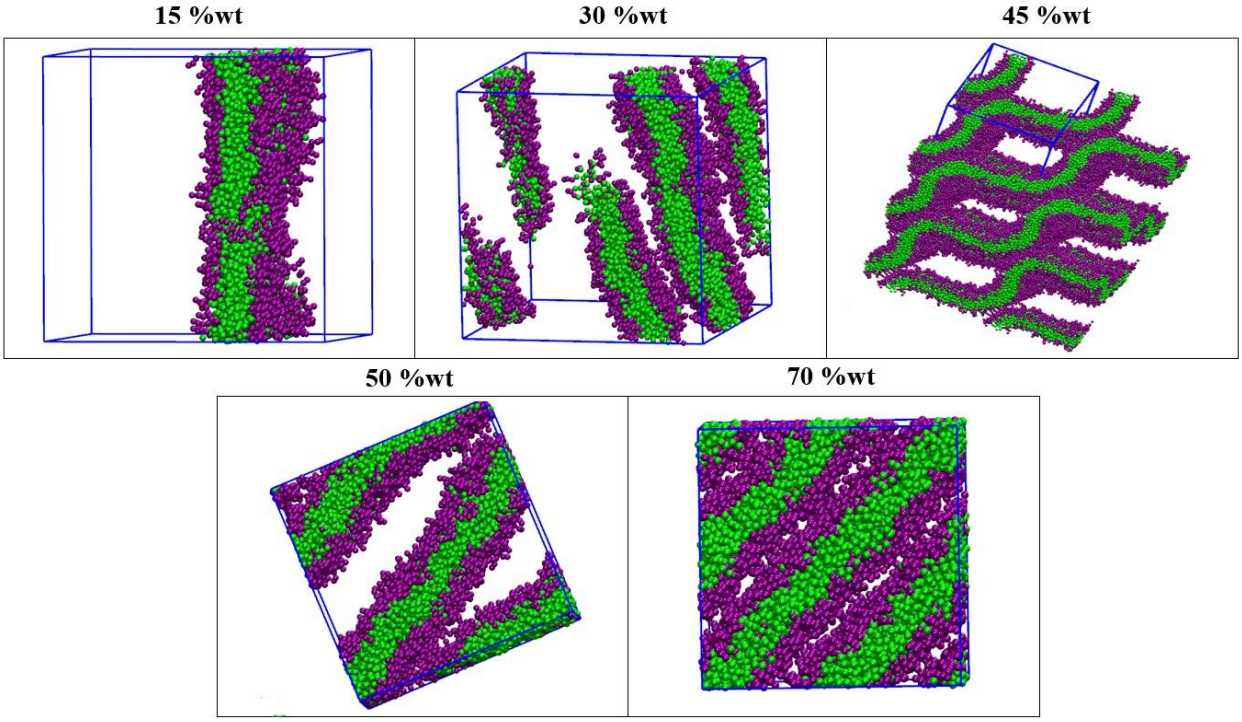


**Figure 2.** CG-MD simulations for $C_{12}E_2$ in water. Green represents the alkyl tail beads, while purple is used to represent the beads of the EO hydrophilic moiety. Water molecules are omitted for a clear visualization.

View Article Online
DOI: 10.1039/D1SM00362C



For $C_{12}E_4$, Mitchell et al.[11] proposed a similar behavior with the system exhibiting a W + $L_\alpha$ dispersion at lower surfactant concentrations and a single $L_\alpha$ in the range of 25-75 %wt. The increased EO units in $C_{12}E_4$ promoted that $V_2$ phases are no longer observed. This system was previously modelled through CG-MD simulations by Rossi et al.[31] and Grunewald et al.[36] but only at 53 %wt of surfactant for which, a defected lamellar phase ($L_\alpha^H$) was observed, i.e. the bilayers contain water-filled defects in the form of pores or necks.[58] In our simulations, displayed in **Figure S5** in Supporting Information, this phase was found at 53 %wt persisting up to at least 70 %wt of surfactant concentration. Only above 80 %wt, near the upper concentration limit for which it was reported in literature, a perfect lamellar phase was observed.

Curiously, as can be observed in the same figure, at lower surfactant concentrations, disperse rod-like micelles are found in solution, instead of the W + $L_\alpha$ dispersion suggested by Mitchell et al.[11] Nevertheless, although the model was not able to reproduce the $L_\alpha$ phase at low surfactant concentrations, as happens for the $C_{12}E_2$, it still predicts a lower surface curvature and the consequent inability of the system to produce spherical micelles for a surfactant with such a low HLB.

Clunie et al.[19] reported the phase diagram for the aqueous solution of $C_{12}E_6$ exhibits a $L_1/H_1/L_\alpha$ sequence. The proposed phase diagram shows an unusual region of micellar phase $L_1$ between $H_1$ and the $L_\alpha$. However, this was not supported by Mitchell et al.[11] in a later study that reported the archetypical sequence of $L_1/H_1/V_1/L_\alpha$ phases. In previous studies using CG-MD simulations, only the $L_1$ and $H_1$ phases were observed. Thus, in this work, the concentration screening allowed to investigate the formation of all the reported phases, as depicted in **Figure 3**. The increased hydrophilicity of the $C_{12}E_6$ yielded a micellar solution at 15 %wt, with the micelles adopting a near spherical shape, contrarily to what it was observed for the lower HLB surfactant $C_{12}E_4$. At 30 %wt, the micelles are larger and adopted a rod-like shape that are at the origin of the cylindrical rods that later form the $H_1$-like phase observed at 50 %wt, in excellent agreement with the experiments.[19]

In contrast, our simulation at 70 %wt (333 K) revealed the formation of a lamellar phase containing water-filled pore defects, as previously observed for the $C_{12}E_4$ system. According to Mitchell and co-workers,[11] at this concentration range, the expected phase can be either $L_\alpha$ or $V_1$ depending on temperature. Therefore, and since the $L_\alpha^H$ is a transition towards $L_\alpha$, we carried out an additional simulation at a lower temperature (303 K). In **Figure 3**, it can be noticed an

View Article Online
DOI: 10.1039/D1SM00362C



intermediate $V_1$-like phase with different layers still connected. Despite the limitation of capturing the effect of temperature in CG-MD simulations, the $V_1 \rightarrow L_\alpha$ transition was indeed promoted by a temperature increase, in agreement with experiments. This is not the usual case, especially when dealing with the $I_1$ and the $H_1$-like phases. The energy barriers during the mesophase formation in CG-MD simulations, usually prevent the system to reach the proper equilibrium state unless higher simulation temperatures are considered. This was previously discussed by us for the phase behavior of imidazolium based ILs.[42]

The presence of a defected lamellar phase in $C_iE_j$/water systems, as found in our simulations, seems to be the most stable phase for the $C_{12}E_6$/water system at around 70 %wt concentration. The defected lamellar phase was first reported for $C_{22}E_6$,[59] $C_{16}E_6$,[50] and $C_{30}E_9$[60] systems and thought to be induced by the increased alkyl chain lengths with limited flexibility, as a way to increase the EO hydration, without changing the surface area per molecule. However, a few years later, Constantin et al.[58] demonstrated that such phase also occurs for surfactants with lower alkyl chains, namely $C_{12}E_6$, at around 65 %wt, in a remarkable agreement with the CG-MD simulations carried out in this work.

Since the $L_\alpha$ phase appeared at even higher surfactant concentrations (up to 85 %wt), an additional simulation at 80 %wt was carried out for this system. The final simulation snapshot is displayed in **Figure 3**, revealing the formation of a defect-free $L_\alpha$ phase. This is in excellent agreement with the work of Mitchell et al,[11] with all the four different phases being observed in our CG-MD simulations.

View Article Online
DOI: 10.1039/D1SM00362C



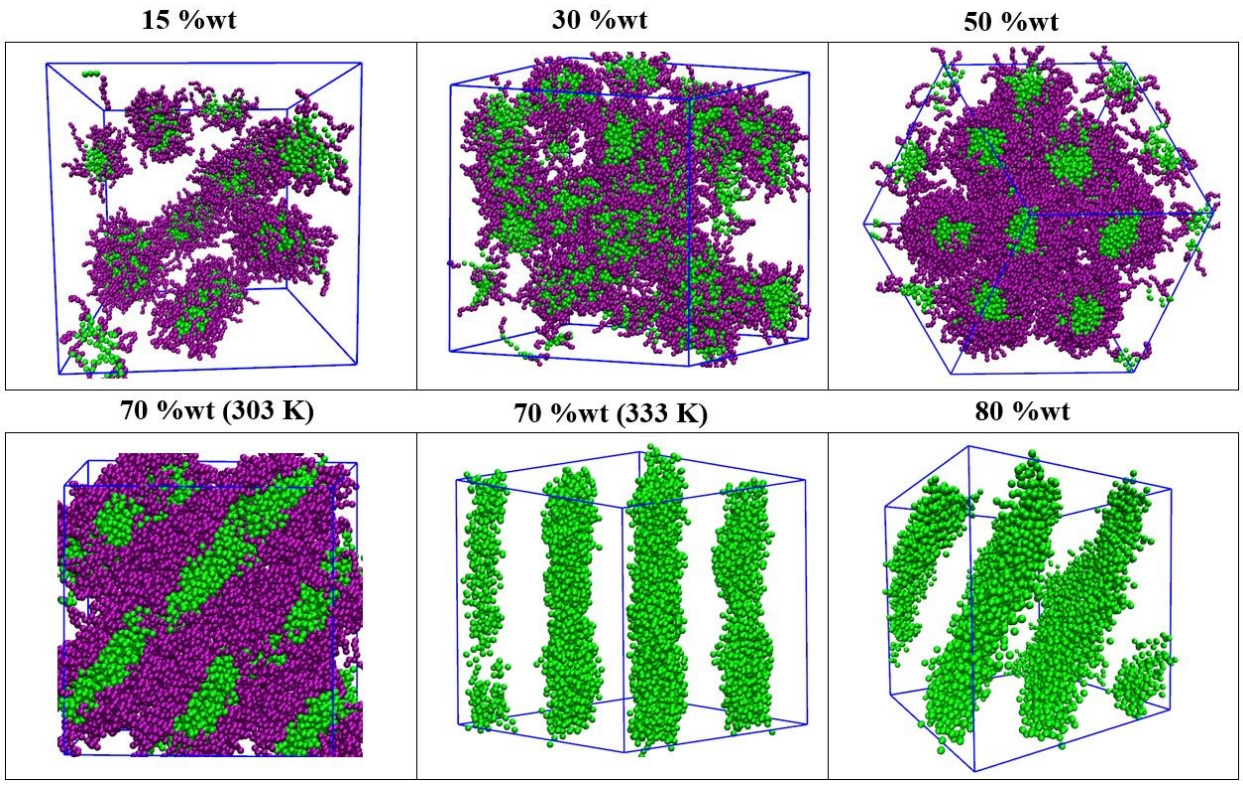


**Figure 3.** CG-MD simulations for aqueous solutions of $C_{12}E_6$ at different surfactant concentrations. Green represents the alkyl tail beads, while purple is used to represent the beads of the EO hydrophilic moiety. Water molecules are omitted for a clear visualization.

It must be noticed that the model correctly captured the structure and formation of the $L_\alpha$ phase for this $C_{12}E_6$ system, a phase that was not observed clearly for $C_8E_6$. This can be ascribed to the increased interactions between alkyl chains and demonstrates the ability of the model to capture the delicate balance of forces required for the formation of the $L_\alpha$ phase.

A further increase in the number of EO units to 10, revealed a decrease in the stability of the lamellar $L_\alpha$ phase. As a consequence, Patrick et al.[48] suggested that, depending on the surfactant concentration, the $C_{12}E_{10}$/water system is either in a micellar solution or in a $H_1$ phase. Our CG-MD simulations, shown in **Figure S6** in Supporting Information, suggest that the model is able to capture such effect for concentrations below 50 %wt, revealing the presence of micelles whose shape and size is varies when the surfactant concentration is increased (spherical micelles → micelle rods → long cylindrical rods). The elongated cylindrical micelles observed at 50 %wt revealed the initial stages of the $H_1$ phase formation, later observed at 70 %wt, in excellent agreement with literature as shown in **Figure 4**. When the surfactant concentration is further

View Article Online
DOI: 10.1039/D1SM00362C



increased to 85 %wt, the CG-MD simulations predicted the formation of a $V_1$ phase. Although this $V_1$ phase was not reported experimentally, it is a well-known feature of this type of systems, being, according to experimental results, also present in $C_{12}E_8$ and, in a very narrow range of conditions, in the $C_{12}E_9$ system.[22,61] It must be pointed out that the $L_\alpha$ phase was not observed in our CG-MD simulations for the $C_{12}E_{10}$/water system, confirming the absence of such phase, as previously reported experimentally for the $C_{12}E_9$ system.[61]

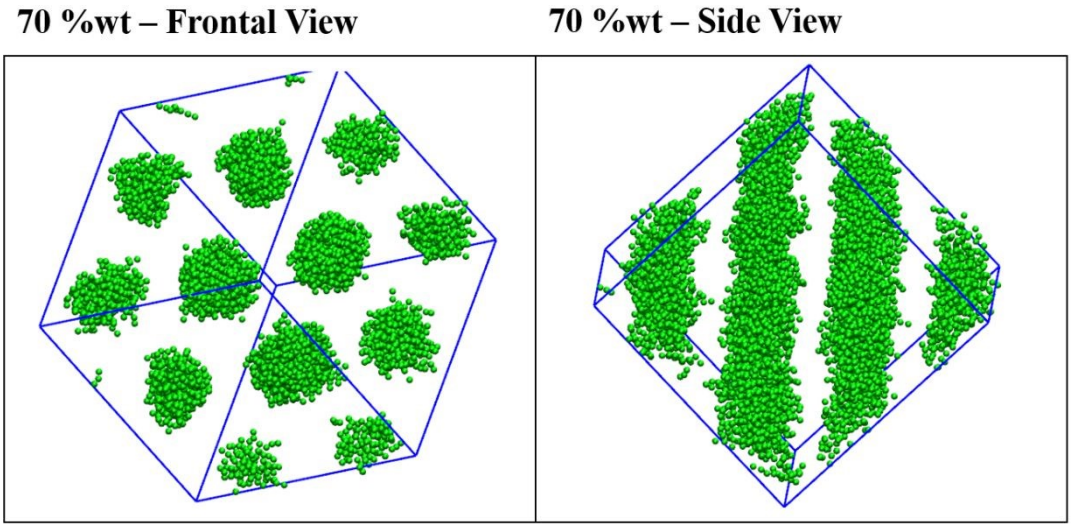


**Figure 4.** Spatial organization of the alkyl tails in the $H_1$ phase observed in the $C_{12}E_{10}$/water system at 70 %wt concentration.

Continuing the trend of decreasing the stability of the lamellar phase, the $C_{12}E_{12}$/water system showed a similar behavior with the exception that, contrarily to $C_{12}E_{10}$, POM observations and low angle X-ray studies carried out by Mitchell et al.[11] revealed the formation of a cubic phase with two different morphologies in the 30-55 %wt concentration range, prior to the formation of the $H_1$ phase. A subsequent study developed by Sakya et al,[49] reinforced the results of Mitchell et al.[11] but stressed the existence of a third morphology of the cubic phase in a very narrow range of temperature and concentration conditions. The results of our CG-MD simulations for the $C_{12}E_{12}$ system are presented in **Figure 5**, confirming the decrease in the stability of the lamellar phase. At 15 %wt, the model predicted the formation of a micellar phase with near-spherical micelles in good agreement with the phase diagram reported by Sakya et al.[49] According to this study, at higher concentrations, a cubic phase with different structures is

View Article Online
DOI: 10.1039/D1SM00362C



expected but such well-defined cubic phases could not be well reproduced by the model. At 50 %wt, cylindrical rod micelles were found instead, that represent the precursor of the $H_1$ phase at this concentration and found to persist up to higher surfactant concentrations. In agreement, in the CG-MD simulation at 70 %wt, a $H_1$ phase is predicted by the model. A further increase of the surfactant concentration (82 %wt) does not lead to a clear $L_\alpha$ phase. Instead, at this concentration, the system seems to be in an intermediate phase between $H_1$ and a $L_\alpha^H$-like phase, similarly to what was observed for $C_{12}E_{10}$.

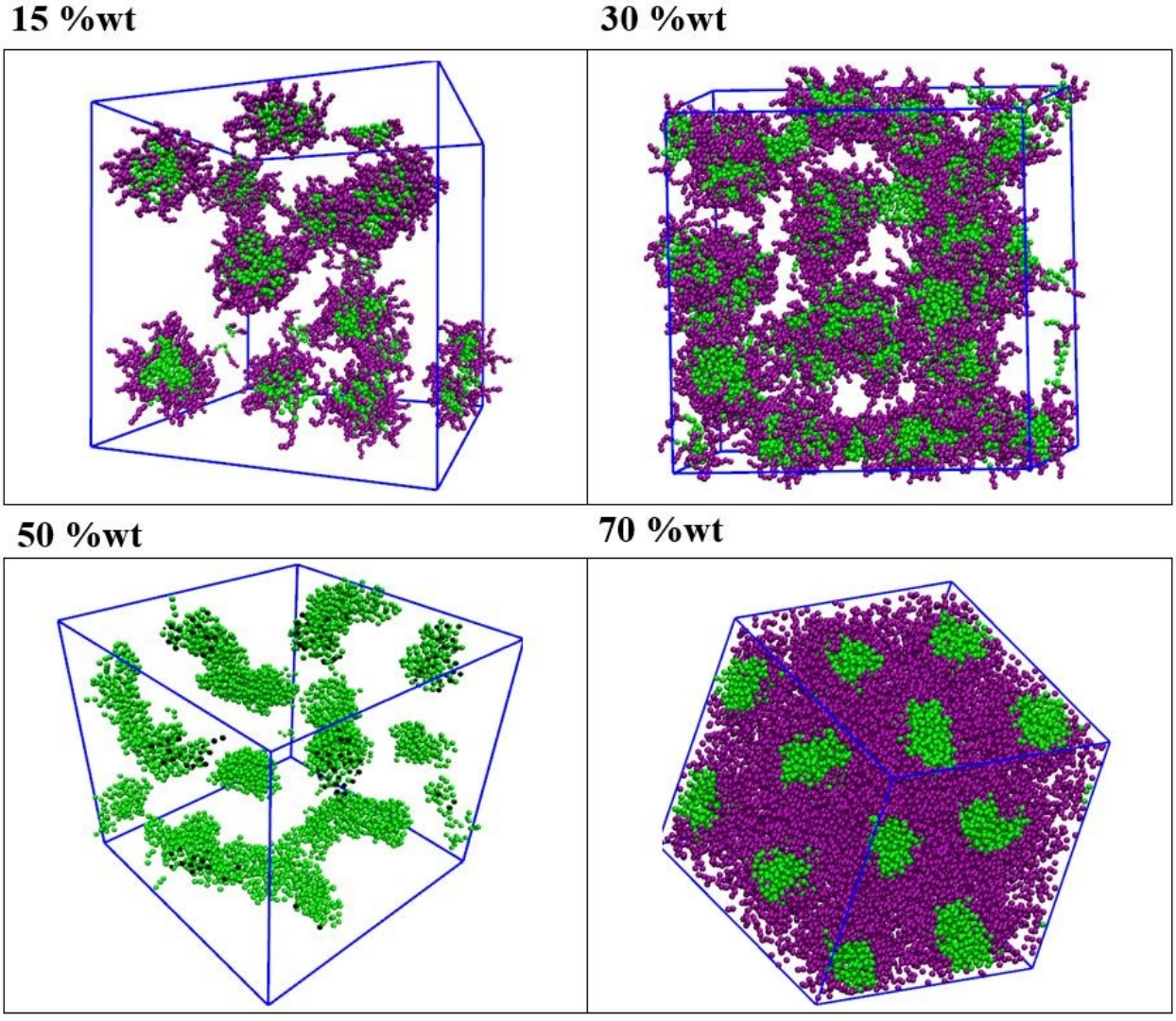


**Figure 5.** CG-MD simulations carried out for $C_{12}E_{12}$/water system at different concentrations. Green represents the alkyl tail beads, while purple is used to represent the beads of the EO hydrophilic moiety. Water molecules are omitted for a clear visualization.

View Article Online
DOI: 10.1039/D1SM00362C



Among the twelve different surfactants analyzed in this work, the $C_{12}E_{23}$ represents the molecule with the highest number of EO units (highest HLB). Due to the increased hydrophilicity, Patrick et al.[48] reported the absence of mesophases in $C_{12}E_{23}$ except for the formation of the $I_1$ phase, although no temperature and concentration ranges data were provided. Our CG-MD simulations for this surfactant confirmed the lack of ordered phases. Instead, a random dispersion of spherical or rod-like micelles (depending on the concentration) was observed in all simulations as illustrated in **Figure S7** in Supporting Information. In fact, even for very high concentrations (e.g., 50 or 70 %wt), most of the micelles retain its sphericity, contrarily to what is observed for surfactants with a lower HLB.

Overall, the results predicted for $C_{12}$ surfactants showed a good agreement with literature reports, especially considering the coarse-grained nature of the model and its inherent transferability. Previous models could not reproduce the phase behavior of surfactants with a considerable number of EO units. Nevertheless, the MARTINI FF successfully provided a reasonable description of $C_iE_j$ surfactants with EO groups up to 23 units. Moreover, the model was able to predict the inability to form spherical micelles when the number of EO units is low ($j$ = 2, 4) as well as how the lamellar phase is the most stable phase for such surfactants. Simultaneously, the model was able to predict how the increased hydrophilicity first induces the instability of the lamellar phase and, then the hexagonal phase emerges for even larger hydrophilic heads. In summary for $C_{12}E_j$ surfactants, increasing $j$, and consequently the HLB, changes the first mesophase from lamellar to hexagonal, and possibly to a cubic-like phase or a micellar solution. This is in good agreement with experiments and the model seems to predict that, as the size and consequently the area occupied by the hydrophilic group is increased, the surfactant packing favors the formation of curved interfaces (spheres and cylinders) over planar ones (bilayers) both observed in the simulations and in the experimental data reported in the literature.

### 3.3. $C_{16}$ surfactants

Previous CG-MD studies of aqueous solutions covering $C_iE_j$ surfactants were restricted to $i$ = 12 and three different EO groups, $j$ = 2, 4, 6. Bearing in mind the effect that longer alkyl chains could have in the mesophase behavior, a set of CG-MD simulations were carried out for $C_{16}$ surfactants with different number of EO units.

View Article Online
DOI: 10.1039/D1SM00362C



Mitchell et al.[11] reported the phase diagram for $C_{16}E_4$. At low surfactant concentrations and temperatures lower than 333 K, the system exhibits a W + $L_\alpha$ dispersion with the $L_\alpha$ phase being replaced by an $L_3$, $V_2$ or $L_2$ phase when the temperature is increased. Such phases are stable up to circa 60 %wt of surfactant, concentration beyond which the lamellar phase is always the most stable phase.

The CG-MD simulation results for $C_{16}E_4$ are presented in **Figure 6**, exhibiting elongated or rod-like micelles at 15 %wt. At 30%wt, the system seems to be in a transition state resembling the $V_1$ phase that often acts as a precursor for layer-like structures such as those later observed at 50 %wt. Despite this intermediate phase was not reported by Mitchell et al.[11], it is compatible with a phase transition from the micellar rods-to-$L_\alpha$ phase observed at low concentrations. This is unequivocally the most stable phase at higher concentrations, and is also observed in our CG-MD simulation at 70 %wt.

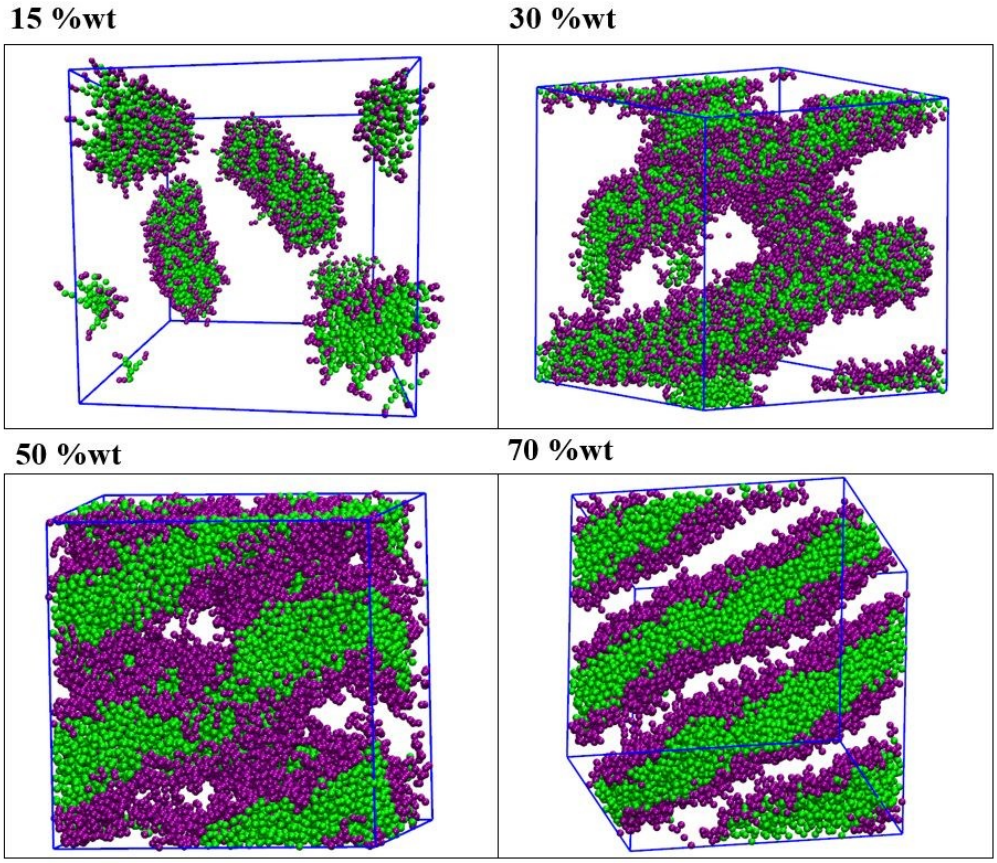


**Figure 6.** Final snapshots of the CG-MD simulations for $C_{16}E_4$ at different concentrations. Green represents the alkyl tail beads, while purple is used to represent the beads of the EO hydrophilic moiety. Water molecules are omitted for a clear visualization.

View Article Online
DOI: 10.1039/D1SM00362C



Funari et al.[50] and Fairhurst et al.[51] reported the phase diagram for the $C_{16}E_6$/water system. Even though there are a few differences concerning the location of the phase boundaries, both studies denoted the presence of an intermediate phase, a term used here for the first time to characterize non-cubic phases between $H_1$ and Lα occurring in $C_iE_j$/water systems. Prior to the formation of the $L_\alpha$ phase, and because long alkyl tails cannot pack into $V_1$ structures,[50] the presence of both, the intermediate phase and a defected lamellar phase $L_\alpha^H$, are expected to arise instead, stressing the role played by the alkyl chain conformations in controlling the transition between $H_1$ and Lα. The CG-MD simulations for the $C_{16}E_6$/water system showed the change in the organization of the alkyl chains due to the increase on the surfactant concentration as presented in **Figure 7**. At 40 %wt, the system formed cylindrical rods resembling the $H_1$ phase that was reported between 35-45 %wt of surfactant concentration.[50,51] At 50 %wt, the system assembled in a mesh-like structure which is one of the possible structures suggested by Holmes and co-workers[51,62] for the intermediate phase, thought to replace $V_1$ for surfactants with considerably long alkyl chains. At higher surfactant concentration, the alkyl chains are already forming a $L_\alpha$ phase with an almost negligible presence of water-filled defects. Although the formation of a defected lamellar phase is expected between the intermediate phase and the Lα, the considerably high temperature and the high concentration contributed to the decreased number of defects found in the $L_\alpha^H$ phase. In **Figure S8** in Supporting Information, another perspective of the simulation box for the 70 %wt system is shown, where one of the pore defects still present can be more easily observed.

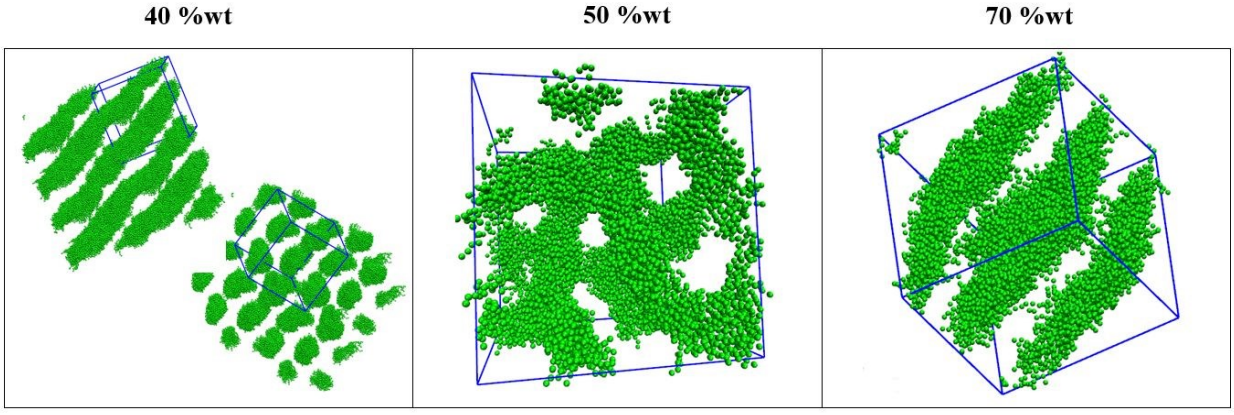


**Figure 7.** Arrangement of the alkyl tails in the $C_{16}E_6$/water system as a function of the surfactant concentration.

View Article Online
DOI: 10.1039/D1SM00362C



It must be highlighted that the model was able to predict the existence of a mesh-like intermediate phase, instead of the typical $V_1$ phase due to the increase of the alkyl chain length, and a relatively low HLB is yet another beacon of the model prediction ability and transferability.

Mitchell et al.[11] reported a few years earlier that neither the intermediate or $L_\alpha^H$ phases were present in $C_{16}E_8$. Instead, the phase diagram displayed the archetypical progression of phases from low to high amphiphile concentrations, *i.e.*, micellar solution → micellar cubic phase → hexagonal columnar phase → bi-continuous cubic phase → lamellar phase. The CG-MD simulations results for this $C_{16}E_8$ system are shown in **Figure 8**. The results display a fair agreement with experiments: at 15 %wt, the system exhibited a micellar solution with the micelles retaining their sphericity up to 30 %wt. At this concentration, the presence of a cubic phase could not be clearly identified, although some sort of long-range ordering of the micelles, resembling a micellar cubic phase, is visible when compared with the results for other systems at different conditions. At 50 %wt, the hexagonal phase is expected according to the literature but only dispersed cylindrical micelles were found. On the contrary, at 70 %wt and 80 %wt the model is able to predict the occurrence of the $V_1$ and $L_\alpha$ phases, respectively. Perhaps, the most interesting result is that the defected lamellar phase – previously observed for $C_{16}E_6$ – was no longer observed in this system. The model was able to capture the ability of the system to form instead a $V_1$-like phase given a sufficiently large $j/i$ ratio. It is important to stress that $V_1$ structures are difficult to characterize, with the best candidates being extended networks where the chain/water interface has both positive and negative curvatures, as observed in some of our simulations.[63]

View Article Online
DOI: 10.1039/D1SM00362C



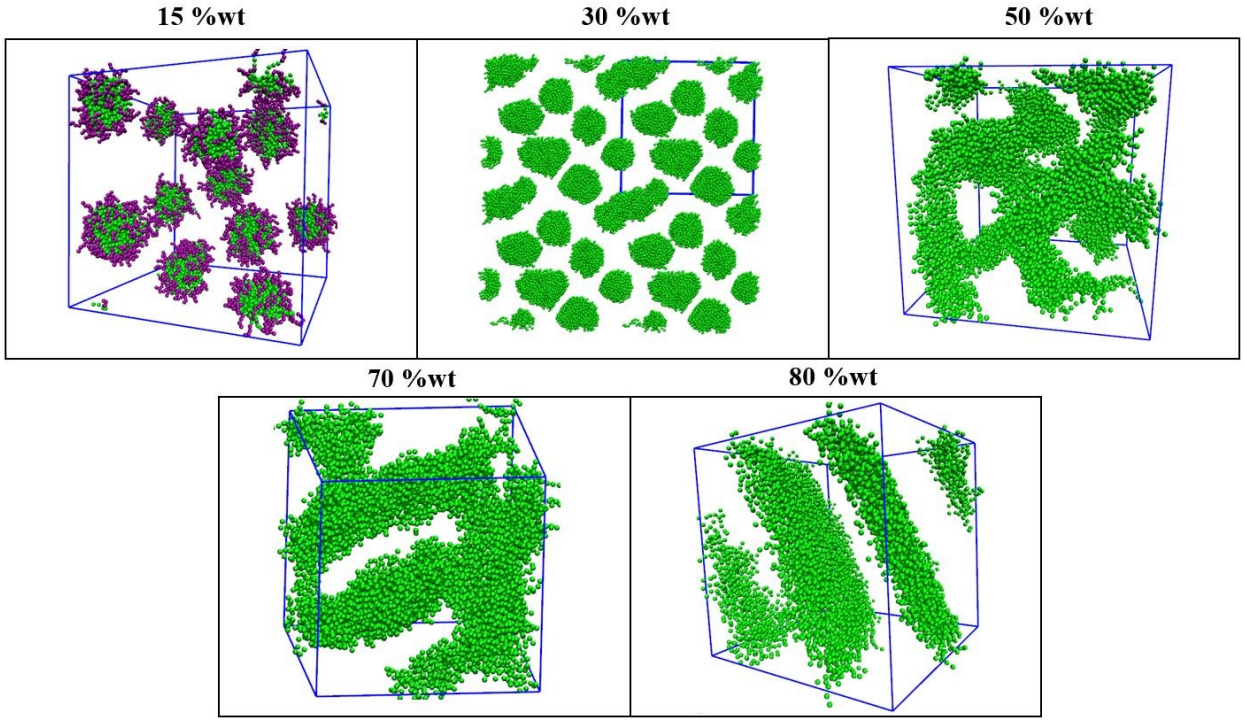


**Figure 8.** Final snapshots of the CG-MD simulations carried out for $C_{16}E_8$/water system. Green represents the alkyl tail beads, while purple is used to represent the beads of the EO hydrophilic moiety. Water molecules are omitted for a clear visualization.

When the number of EO groups are increased, such as in $C_{16}E_{12}$, the agreement with experiments was less satisfactory. According to the work of Mitchell et al.[11] at 30, 50 and 70 %wt the $I_1$, $H_1$, and $V_1/L_\alpha$ phases are expected. The stability of the bi-continuous and lamellar phases decreases considerably and are only present in a very narrow range of concentrations. In our CG-MD simulations, depicted in **Figure S9**, at 30 %wt, the cubic phase was not found and at 50 %wt the cylindrical micelles were somehow organized but not in the expected hexagonal array. At 70 %wt, the bi-continuous cubic phase was observed, as reported in the literature. However, the lamellar phase persisted to even higher concentrations (up to 90%wt) contrary what it was observed experimentally. This is, however, a common issue of MD simulations when tackling phase transitions starting from a lamellar phase at very high concentrations. Nonetheless, the ability of the model to predict the existence of a $V_1$-like phase instead of a defected lamellar phase still a remarkable achievement.

View Article Online
DOI: 10.1039/D1SM00362C



### 3.4. The low concentration regime

At diluted concentrations, a surfactant molecule is usually present in water as a solution of surfactant unimers or small oligomers aggregates. However, at a given temperature, once the surfactant concentration is increased beyond a certain threshold – denoted as the critical micellar concentration (cmc) – small spherical-shaped aggregates are formed to decrease the alkyl chain area exposed to water molecules. By increasing the surfactant concentration, the size of the micelles tends to rise, while its sphericity is severely decreased, leading to the formation of rod-like and disk-like aggregates that can be seen as precursors of long-range ordering phases such as $H_1$ and $L_\alpha$.

Therefore, having a reasonable description of the micellar aggregates, precursors of certain mesophases, and the knowledge on how the cmc or the average micellar aggregation numbers ($N_{agg}$) vary with the surfactant nature, is highly relevant for the design and understanding of $C_iE_j$ solutions. While cmc values are relatively easy to determine experimentally, usually capturing changes in the behavior of one or more physical properties (*e.g.,* conductivity, surface tension, etc.), it is a tough question for MD simulations. This is mainly due to the very low cmc values of non-ionic surfactants when compared to their ionic counterparts that makes it very computational demanding to systematically simulate systems at such low concentrations, even using CG models. The experimental cmc and $N_{agg}$ values found in literature for the studied surfactants are provided in **Table 2**. In the case of the $C_{12}E_6$ aqueous solution – surfactant with an intermediate HLB value in between those studied in this work – the cmc reported experimentally ranges between 6.8 and $8.8 \cdot 10^{-5}$ M, while their $N_{agg}$ are between 110-180.[9,64,65] Considering the highest concentration and the lowest $N_{agg}$, a simulation of only 110 molecules of surfactant requires more than 17 millions of CG water beads (68 millions of water molecules). An alternative is to perform simulations at higher concentrations but still within the micellar phase. Then, the average free surfactant unimer concentration can be used as a rough estimation of the actual cmc. This approach has been previously used with the MARTINI FF, using a different CG mapping for the $C_iE_j$ molecules, and found to provide a reasonable estimation of the cmc values, although an incorrect temperature dependency was observed.[1]

View Article Online
DOI: 10.1039/D1SM00362C



**Table 2.** Micelle aggregation numbers determined from the CG-MD simulations at 15 %wt of surfactant and literature values for $N_{agg}$ and cmc.

| Surfactant | $N_{min}$ | $N_{max}$ | $N_{agg}$ | $N_{agg,Lit}$ | Ref. | $cmc_{Lit}$ (M) | Ref. |
|---|---|---|---|---|---|---|---|
| $C_8E_6$ | 43 | 104 | 61.9 | 32 | 66 | $\sim 9.8 \cdot 10^{-3}$ | 67–69 |
| | | | | 51 | 70 | $7.6 \cdot 10^{-3}$ | 69 |
| | | | | | | $1.68 \cdot 10^{-2}$ | 69 |
| | | | | >300 | 71 | $2.3 \cdot 10^{-4}$ | 65 |
| $C_8E_{12}$ | 34 | 59 | 46.6 | - | | - | |
| $C_{12}E_2$ | - | - | - | - | | $3.3 \cdot 10^{-5}$ | 12 |
| $C_{12}E_4$ | 140 | 329 | 250.0 | 160* | 64 | $6.0 \cdot 10^{-5}$* | 64 |
| | | | | | | $4.33 \cdot 10^{-5}$ | 72 |
| $C_{12}E_6$ | 53 | 158 | 90.9 | 110 | 64 | $6.8 \cdot 10^{-5}$ | 64 |
| | | | | 144-180 | 65 | $8.8 \cdot 10^{-5}$ | 9 |
| $C_{12}E_{10}$ | 38 | 72 | 58.8 | - | | - | |
| $C_{12}E_{12}$ | 29 | 70 | 50.0 | 81 | 65 | $1.4 \cdot 10^{-4}$ | 12,65 |
| $C_{12}E_{23}$ | 19 | 61 | 38.5 | 40 | 64 | $1.0 \cdot 10^{-4}$ | 64 |
| | | | | 41 | 65 | $1.75 \cdot 10^{-4}$ | 65 |
| $C_{16}E_4$ | 176 | 322 | 250 | | | | |
| $C_{16}E_6$ | 73 | 168 | 111.1 | | | $1.3 \cdot 10^{-6}$ | 73 |
| $C_{16}E_8$ | 56 | 114 | 83.3 | 160 | 65 | $5.0 \cdot 10^{-7}$ | 74 |
| $C_{16}E_{12}$ | 39 | 105 | 66.7 | 152 | 65 | $2.3 \cdot 10^{-6}$ | 65 |

*values for $C_{12}E_5$
Lit – Literature values

With the aim to explore the ability of the $C_iE_j$ CG model at concentrations near the cmc, an additional simulation of 51 $C_8E_6$ molecules (the surfactant with the lowest cmc from those investigated in this work) was carried out at $9.8 \cdot 10^{-3}$ M. After 5μs of simulation, using an in-house cluster counting code, the $N_{agg}$ was found to be 39 surfactant molecules, with 12 molecules remaining freely in the solution. The free surfactant unimers correspond to a concentration of $2.3 \cdot 10^{-3}$ M that compares reasonably well with the values reported from literature. This fact suggests that the CG mapping proposed by Grunewald et al.,[36] used in our study retains the ability to provide a reasonable estimate of the cmc for $C_iE_j$ surfactants in water.

View Article Online
DOI: 10.1039/D1SM00362C



The MARTINI FF has been previously applied for the prediction of the $N_{agg}$ in aqueous solutions of $C_iE_j$ surfactants[1] and to obtain the average size distribution of ethylene oxide urethane micelles[75]. However, in those works previous parameterizations of the EO groups based on pre-existing MARTINI beads were considered. Therefore, aiming at evaluating the ability of the new EO parameterization to predict the aggregation behavior of CiEj surfactants, the $N_{agg}$ values, were here obtained using an in-house cluster counting code for the systems at 15 %wt. It is however important to point out two aspects of the values obtained using this procedure: firstly, the $N_{agg}$ cannot be obtained for the $C_{12}E_2$ system, since the $L_\alpha$ phase was already observed at 15 %wt. Secondly, as $N_{agg}$ tends to increase with surfactant concentration, the values reported here are expected to be slightly higher than those that would have been predicted by the model at the cmc, especially for those surfactants with a considerably high *i* to *j* ratio, where micellar-to-rod transition was observed at this concentration, instead of spherical micelles, observed in $C_{12}E_4$ and $C_{16}E_4$.

The aggregation numbers (minimum, maximum, and average) obtained in the CG-MD simulations are reported in **Table 2** and compared with some experimental values found in the literature. It must be pointed out that the literature values should be taken with caution since diverse values were reported by different authors and, in addition, the concentrations were not always shown. **Table 2** exhibits a considerable disparity between the minimum and maximum micelle size. Conversely, the $N_{agg}$ values obtained correctly describe the effect of the chain length, increasing the $N_{agg}$ with *i* and decreasing with *j*. The agreement with literature can also be considered fairly satisfactory, in particular for $C_8E_6$, $C_{12}E_6$, and $C_{12}E_{23}$ systems. It is worth to highlight the excellent agreement obtained for the $C_{12}E_6$, $N_{agg} \sim 90.9$, which is close to the value reported in literature as shown in **Table 2**, $N_{agg} = 110$, and different to the $N_{agg} = 45$ previously reported by Puvvada et al.[24,76] who they used a molecular thermodynamic approach to predict the micellization.

Clearly, the highest deviations were observed for the $C_{16}$ systems when comparing with the data reported by Levitz et al.[65] however, such data could have been severely overestimated. For instance, in the $C_8E_6$ system, micelles with more than 300 surfactant molecules were reported even though, other authors have reported values between 32 and 51 for the same system[69,77] or 80 for $C_8E_5$, whose $N_{agg}$ is expected to be higher.[64]

View Article Online
DOI: 10.1039/D1SM00362C



These results reinforce the ability of the MARTINI FF to provide a reasonable description of the low concentration micellar regime in aqueous solutions of non-ionic surfactants; however, as previously mentioned, to obtain quantitative measurements of the *cmc* using this type of simulations can easily become computational prohibitive, especially for the longer non-ionic surfactants with very low *cmc* values. One viable alternative, suggested by Anogiannakis et al,[78] is to use an implicit solvent version of the MARTINI FF to calculate such diluted properties, while retaining the original variant to study the phase behavior at higher concentrations. In their work, after a small tweak of the interaction between the hydrophobic beads and of the electric permittivity of water, a good agreement with the *cmc* and $N_{agg}$ of ionic surfactants was achieved and, considering the good description obtained here, similar results can be expected for the non-ionic surfactants. Another alternative would be to adapt the methodology proposed by Santos et al.[79] that used Monte Carlo simulations of a lattice surfactant model to determine the *cmc* from extrapolations of the unimer surfactant concentration. However, as exemplified above for $C_{12}E_6$, diluted simulations of these surfactants at concentrations even slightly above the *cmc* are computational prohibitive so that an implicit solvent model would still be required.[79]

A final model benchmark on describing the diluted region of the $C_iE_j$/water systems is the micellar radius. Unfortunately, experimental data was only found for $C_{12}E_6$, exhibiting a micelle radius ~ 20 ± 5 Å reported by Corti et al.[9] To obtain the micelle radius from the CG-MD simulation carried out for $C_{12}E_6$/water system at 15 %wt, the micelle density profile from the micelle center of mass was obtained and shown in **Figure 9**. The micelle radius is the distance from the center of the micelle (0) to the maximum of hydrophilic head curve (purple). Thus, the micellar radius is ~21.7 Å which is in excellent agreement with the literature. This suggests that the model correctly describes the molecular packing of the surfactant within the micelles.

View Article Online
DOI: 10.1039/D1SM00362C



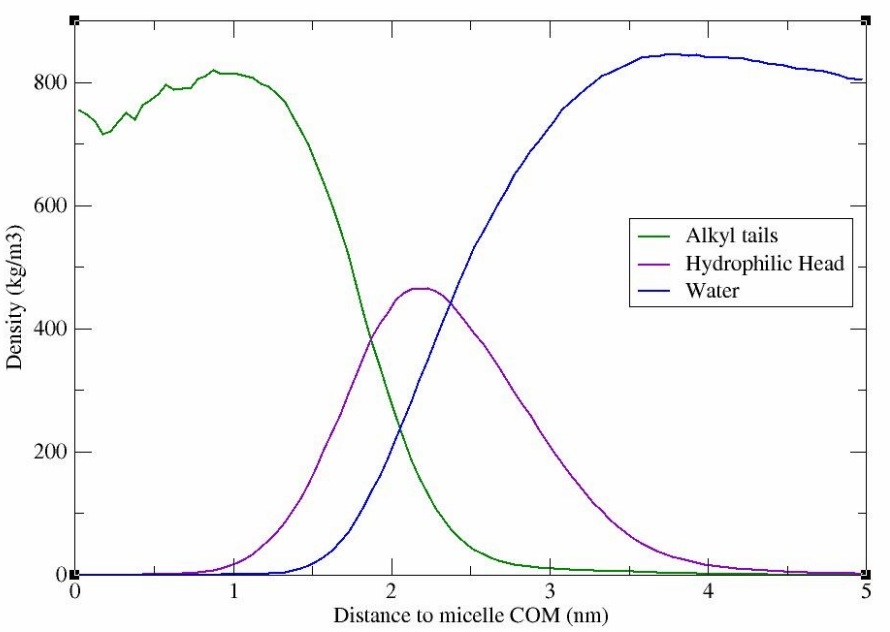


**Figure 9.** Micelle density profile for the $C_{12}E_6$ in water as obtained from the CG-MD simulation at 15 %wt.

## 4. Conclusions

In this work, an extensive analysis of the influence of molecular structure and concentration on the phase behavior of aqueous solutions of $C_iE_j$ surfactants was carried out using a MARTINI FF for CG-MD simulations. Twelve different surfactants with different chain lengths of both the hydrophobic and hydrophilic moieties were investigated at different concentrations, allowing to span a wide range of HLB values.

Concerning the effect of the alkyl chain length, MD simulations were able to correctly reproduce how an increase of *i* from 8 to 12 leads to the decrease of mesophase instability. LC phases were obtained for $C_{12}$ surfactants, even for small hydrophilic moieties, for which a lamellar phase can be predicted even at very low surfactant loadings, in agreement with experiments. In addition, the effect of adding EO units is shown to be well captured by the model, used to simulate surfactants with up to 23 EO units, accurately describing the decreased stability of the lamellar phase when the number of EO chains are increased.

In terms of mesophase structures, the model captured the existence of intermediate phases between $H_1$ and $L_\alpha$, other than the usual $V_1$ phases, typical of these types of systems. As an

View Article Online
DOI: 10.1039/D1SM00362C



example, the presence of a defected lamellar phase, initially supposed to exist only for long alkyl chains ($i > 16$), was here shown also for $C_{12}$ surfactants, in excellent agreement with some of the most recent studies.

Furthermore, the model provided a reasonable description of the micellar regime, namely the micelle radius, aggregation numbers and critical micellar concentration, in agreement with experiments, considering the uncertainty of some experimental values.

Overall, the model correctly predicted the formation of LC phases in $C_iE_j$ systems in a wide range of concentrations in good agreement with experiments, regardless the surfactant structure, while still providing a reasonable description of diluted micellar phases. The obtained results improve the reliability of the MARTINI $C_iE_j$ model, paving the way for the use in multi-component systems used in the industry and diverse research areas, providing some clues when experimental data is not available.

## CRediT authorship contribution statement

Emanuel A. Crespo – Investigation, Visualization, Data Curation, Writing – original draft; Lourdes F. Vega – Supervision, Validation, Writing- review & editing.
Germán Pérez-Sánchez – Conceptualization, Investigation, Validation, Writing- original draft; João A. P. Coutinho – Funding Acquisition, Conceptualization, Supervision, Writing – review & editing.

## Acknowledgments

This work was developed within the scope of the projects CICECO-Aveiro Institute of Materials, UIDB/50011/2020 & UIDP/50011/2020 and SILVIA ref. CENTRO-01-0145-FEDER-31002 financed by national funds through the FCT/MEC and when appropriate co-financed by FEDER under the PT2020 Partnership Agreement. E. A. Crespo acknowledges FCT for the Ph.D. Grant SFRH/BD/130870/2017. German Perez-Sanchez acknowledges the national funds (OE), through FCT – Fundação para a Ciência e a Tecnologia, I.P., in the scope of the framework contract foreseen in the numbers 4, 5 and 6 of the article 23, of the Decree-Law 57/2016, of August 29, changed by Law 57/2017, of July 19. L. F. Vega acknowledges partial financial support by Khalifa University of Science and Technology under project RC2-2019-007.

View Article Online
DOI: 10.1039/D1SM00362C



## References


1 S. A. Sanders and A. Z. Panagiotopoulos, Micellization behavior of coarse grained surfactant models, *J. Chem. Phys.*, 2010, **132**, 114902.

2 C. Cowan-Ellsberry, S. Belanger, P. Dorn, S. Dyer, D. McAvoy, H. Sanderson, D. Versteeg, D. Ferrer and K. Stanton, Environmental Safety of the Use of Major Surfactant Classes in North America, *Crit. Rev. Environ. Sci. Technol.*, 2014, **44**, 1893–1993.

3 T. M. Ferreira, D. Topgaard and O. H. S. Ollila, Molecular Conformation and Bilayer Pores in a Nonionic Surfactant Lamellar Phase Studied with 1H–13C Solid-State NMR and Molecular Dynamics Simulations, *Langmuir*, 2014, **30**, 461–469.

4 J. Eastoe and R. F. Tabor, in *Colloidal Foundations of Nanoscience*, eds. D. Berti and G. Palazzo, Elsevier, Amsterdam (The Netherlands), 2014, pp. 135–157.

5 K. Holmberg, B. Jonsson, B. Kronberg and B. Lindman, *Surfactants and Polymers in Aqueous Solutions*, John Wiley & Sons, Hoboken, NJ, 2nd edn., 2003.

6 J.-H. Ryu, S. Park, B. Kim, A. Klaikherd, T. P. Russell and S. Thayumanavan, Highly Ordered Gold Nanotubes Using Thiols at a Cleavable Block Copolymer Interface, *J. Am. Chem. Soc.*, 2009, **131**, 9870–9871.

7 S. Garde, L. U. Yang, J. S. Dordick and M. E. Paulaitis, Molecular dynamics simulation of C8E5 micelle in explicit water: structure and hydrophobic solvation thermodynamics, *Mol. Phys.*, 2002, **100**, 2299–2306.

8 G. T. Dimitrova, T. F. Tadros and P. F. Luckham, Investigations of the Phase Changes of Nonionic Surfactants Using Microscopy, Differential Scanning Calorimetry, and Rheology. 1. Synperonic A7, a C13/C15 Alcohol with 7 mol of Ethylene Oxide, *Langmuir*, 1995, **11**, 1101–1111.

9 M. Corti and V. Degiorgio, Critical Behavior of a Micellar Solution, *Phys. Rev. Lett.*, 1980, **45**, 1045–1048.

10 M. Zulauf and J. P. Rosenbusch, Micelle clusters of octylhydroxyoligo(oxyethylenes), *J. Phys. Chem.*, 1983, **87**, 856–862.

11 D. J. Mitchell, G. J. T. Tiddy, L. Waring, T. Bostock and M. P. McDonald, Phase behaviour of polyoxyethylene surfactants with water. Mesophase structures and partial miscibility (cloud points), *J. Chem. Soc. Faraday Trans. 1 Phys. Chem. Condens. Phases*, 1983, **79**, 975–1000.

View Article Online
DOI: 10.1039/D1SM00362C



12 R. Dong and J. Hao, Complex Fluids of Poly(oxyethylene) Monoalkyl Ether Nonionic Surfactants, *Chem. Rev.*, 2010, **110**, 4978–5022.

13 Y. Nibu and T. Inoue, Phase Behavior of Aqueous Mixtures of Some Polyethylene Glycol Decyl Ethers Revealed by DSC and FT-IR Measurements, *J. Colloid Interface Sci.*, 1998, **205**, 305–315.

14 J. C. Lang and R. D. Morgan, Nonionic surfactant mixtures. I. Phase equilibria in C10E4–H2O and closed-loop coexistence, *J. Chem. Phys.*, 1980, **73**, 5849–5861.

15 B. A. Mulley and A. D. Metcalf, Nonionic surface-active agents. Part VI. Phase equilibria in binary and ternary systems containing nonionic surface-active agents, *J. Colloid Sci.*, 1964, **19**, 501–515.

16 J. S. Clunie, J. M. Corkill, J. F. Goodman, P. C. Symons and J. R. Tate, Thermodynamics of non-ionic surface-active agent + water systems, *Trans. Faraday Soc.*, 1967, **63**, 2839–2845.

17 S. S. Funari and G. Rapp, X-ray Studies on the C12EO2/Water System, *J. Phys. Chem. B*, 1997, **101**, 732–739.

18 M. L. Lynch, K. A. Kochvar, J. L. Burns and R. G. Laughlin, Aqueous-Phase Behavior and Cubic Phase-Containing Emulsions in the C12E2−Water System, *Langmuir*, 2000, **16**, 3537–3542.

19 J. S. Clunie, J. F. Goodman and P. C. Symons, Phase equilibria of dodecylhexaoxyethylene glycol monoether in water, *Trans. Faraday Soc.*, 1969, **65**, 287–296.

20 K. Shinoda, Thermodynamic aspects of nonionic surfactant—Water systems, *J. Colloid Interface Sci.*, 1970, **34**, 278–282.

21 V. Degiorgio, R. Piazza, M. Corti and C. Minero, Critical properties of nonionic micellar solutions, *J. Chem. Phys.*, 1985, **82**, 1025–1031.

22 E. Jahns and H. Finkelmann, Lyotropic liquid crystalline phase behavior of a polymeric amphiphile polymerized via their hydrophilic ends, *Colloid Polym. Sci.*, 1987, **265**, 304–311.

23 F. Sterpone, G. Briganti and C. Pierleoni, Molecular Dynamics Study of Spherical Aggregates of Chain Molecules at Different Degrees of Hydrophilicity in Water Solution, *Langmuir*, 2001, **17**, 5103–5110.

View Article Online
DOI: 10.1039/D1SM00362C



24 F. Sterpone, C. Pierleoni, G. Briganti and M. Marchi, Molecular Dynamics Study of Temperature Dehydration of a C12E6 Spherical Micelle, *Langmuir*, 2004, **20**, 4311–4314.

25 C. Senac, W. Urbach, E. Kurtisovski, P. H. Hünenberger, B. A. C. Horta, N. Taulier and P. F. J. Fuchs, Simulating Bilayers of Nonionic Surfactants with the GROMOS-Compatible 2016H66 Force Field, *Langmuir*, 2017, **33**, 10225–10238.

26 H. Lee, R. M. Venable, A. D. MacKerell and R. W. Pastor, Molecular Dynamics Studies of Polyethylene Oxide and Polyethylene Glycol: Hydrodynamic Radius and Shape Anisotropy, *Biophys. J.*, 2008, **95**, 1590–1599.

27 W. Shinoda, R. DeVane and M. L. Klein, Multi-property fitting and parameterization of a coarse grained model for aqueous surfactants, *Mol. Simul.*, 2007, **33**, 27–36.

28 W. Shinoda, R. DeVane and M. L. Klein, Coarse-grained molecular modeling of non-ionic surfactant self-assembly, *Soft Matter*, 2008, **4**, 2454–2462.

29 M. Velinova, D. Sengupta, A. V Tadjer and S.-J. Marrink, Sphere-to-Rod Transitions of Nonionic Surfactant Micelles in Aqueous Solution Modeled by Molecular Dynamics Simulations, *Langmuir*, 2011, **27**, 14071–14077.

30 M. Velinova, Y. Tsoneva, A. Ivanova and A. Tadjer, Estimation of the Mutual Orientation and Intermolecular Interaction of C12Ex from Molecular Dynamics Simulations, *J. Phys. Chem. B*, 2012, **116**, 4879–4888.

31 G. Rossi, P. F. J. Fuchs, J. Barnoud and L. Monticelli, A Coarse-Grained MARTINI Model of Polyethylene Glycol and of Polyoxyethylene Alkyl Ether Surfactants, *J. Phys. Chem. B*, 2012, **116**, 14353–14362.

32 M. Vuorte, J. Määttä and M. Sammalkorpi, Simulations Study of Single-Component and Mixed n-Alkyl-PEG Micelles, *J. Phys. Chem. B*, 2018, **122**, 4851–4860.

33 T. Taddese and P. Carbone, Effect of Chain Length on the Partition Properties of Poly(ethylene oxide): Comparison between MARTINI Coarse-Grained and Atomistic Models, *J. Phys. Chem. B*, 2017, **121**, 1601–1609.

34 S. J. Marrink, H. J. Risselada, S. Yefimov, D. P. Tieleman and A. H. de Vries, The MARTINI Force Field: Coarse Grained Model for Biomolecular Simulations, *J. Phys. Chem. B*, 2007, **111**, 7812–7824.

35 V. Adrien, G. Rayan, M. Reffay, L. Porcar, A. Maldonado, A. Ducruix, W. Urbach and N. Taulier, Characterization of a Biomimetic Mesophase Composed of Nonionic Surfactants

View Article Online
DOI: 10.1039/D1SM00362C



and an Aqueous Solvent, *Langmuir*, 2016, **32**, 10268–10275.

36 F. Grunewald, G. Rossi, A. H. de Vries, S. J. Marrink and L. Monticelli, Transferable MARTINI Model of Poly(ethylene Oxide), *J. Phys. Chem. B*, 2018, **122**, 7436–7449.

37 M. J. Abraham, T. Murtola, R. Schulz, S. Páll, J. C. Smith, B. Hess and E. Lindahl, GROMACS: High performance molecular simulations through multi-level parallelism from laptops to supercomputers, *SoftwareX*, 2015, **1**–**2**, 19–25.

38 M. Bulacu, N. Goga, W. Zhao, G. Rossi, L. Monticelli, X. Periole, D. P. Tieleman and S. J. Marrink, Improved Angle Potentials for Coarse-Grained Molecular Dynamics Simulations, *J. Chem. Theory Comput.*, 2013, **9**, 3282–3292.

39 G. Bussi, D. Donadio and M. Parrinello, Canonical sampling through velocity rescaling, *J. Chem. Phys.*, 2007, **126**, 14101.

40 M. Parrinello and A. Rahman, Polymorphic transitions in single crystals: A new molecular dynamics method, *J. Appl. Phys.*, 1981, **52**, 7182–7190.

41 B. Hess, H. Bekker, H. J. C. Berendsen and J. G. E. M. Fraaije, LINCS: A linear constraint solver for molecular simulations, *J. Comput. Chem.*, 1997, **18**, 1463–1472.

42 E. A. Crespo, N. Schaeffer, J. A. P. Coutinho and G. Perez-Sanchez, Improved coarse-grain model to unravel the phase behavior of 1-alkyl-3-methylimidazolium-based ionic liquids through molecular dynamics simulations, *J. Colloid Interface Sci.*, 2020, **574**, 324–336.

43 L. Martínez, R. Andrade, E. G. Birgin and J. M. Martínez, PACKMOL: A package for building initial configurations for molecular dynamics simulations, *J. Comput. Chem.*, 2009, **30**, 2157–2164.

44 W. Humphrey, A. Dalke and K. Schulten, VMD: Visual molecular dynamics, *J. Mol. Graph.*, 1996, **14**, 33–38.

45 G. Pérez-Sánchez, J. R. B. Gomes and M. Jorge, Modeling Self-Assembly of Silica/Surfactant Mesostructures in the Templated Synthesis of Nanoporous Solids, *Langmuir*, 2013, **29**, 2387–2396.

46 J. Hoshen and R. Kopelman, Percolation and cluster distribution. I. Cluster multiple labeling technique and critical concentration algorithm, *Phys. Rev. B*, 1976, **14**, 3438–3445.

47 W. C. Griffin, Calculation of HLB Values of Non-Ionic Surfactants, *J. Soc. Coesmetic*

View Article Online
DOI: 10.1039/D1SM00362C



*Chem.*, 1954, **5**, 249–256.

48 H. N. Patrick and G. G. Warr, Self-assembly structures of nonionic surfactants at graphite–solution interfaces. 2. Effect of polydispersity and alkyl chain branching, *Colloids Surfaces A Physicochem. Eng. Asp.*, 2000, **162**, 149–157.

49 P. Sakya, J. M. Seddon, R. H. Templer, R. J. Mirkin and G. J. T. Tiddy, Micellar Cubic Phases and Their Structural Relationships: The Nonionic Surfactant System C12EO12/Water, *Langmuir*, 1997, **13**, 3706–3714.

50 S. S. Funari, M. C. Holmes and G. J. T. Tiddy, Intermediate Lyotropic Liquid Crystal Phases in the C16EO6/Water System, *J. Phys. Chem.*, 1994, **98**, 3015–3023.

51 C. E. Fairhurst, M. C. Holmes and M. S. Leaver, Structure and Morphology of the Intermediate Phase Region in the Nonionic Surfactant C16EO6/Water System, *Langmuir*, 1997, **13**, 4964–4975.

52 S. P. Christensen, F. A. Donate, T. C. Frank, R. J. LaTulip and L. C. Wilson, Mutual Solubility and Lower Critical Solution Temperature for Water + Glycol Ether Systems, *J. Chem. Eng. Data*, 2005, **50**, 869–877.

53 W. H. Richtering, W. Burchard, E. Jahns and H. Finkelmann, Light scattering from aqueous solutions of a nonionic surfactant (C14E8) in a wide concentration range, *J. Phys. Chem.*, 1988, **92**, 6032–6040.

54 B. Lindman and H. Wennerstroem, Nonionic micelles grow with increasing temperature, *J. Phys. Chem.*, 1991, **95**, 6053–6054.

55 W. G. Chapman, K. E. Gubbins, G. Jackson and M. Radosz, SAFT: Equation-of-state solution model for associating fluids, *Fluid Phase Equilib.*, 1989, **52**, 31–38.

56 W. G. Chapman, K. E. Gubbins, G. Jackson and M. Radosz, New reference equation of state for associating liquids, *Ind. Eng. Chem. Res.*, 1990, **29**, 1709–1721.

57 J. S. Marland and B. A. Mulley, A phase-rule study of multiple-phase formation in a model emulsion system containing water, n-octanol, n-dodecane and/a non-ionic surface-active agent at 10 and 25°, *J. Pharm. Pharmacol.*, 1971, **23**, 561–572.

58 D. Constantin and P. Oswald, Diffusion Coefficients in a Lamellar Lyotropic Phase: Evidence for Defects Connecting the Surfactant Structure, *Phys. Rev. Lett.*, 2000, **85**, 4297–4300.

59 S. S. Funari, M. C. Holmes and G. J. T. Tiddy, Microscopy, x-ray diffraction, and NMR

View Article Online
DOI: 10.1039/D1SM00362C



studies of lyotropic liquid crystal phases in the C22EO6/water system: a new intermediate phase, *J. Phys. Chem.*, 1992, **96**, 11029–11038.

60 J. Burgoyne, M. C. Holmes and G. J. T. Tiddy, An Extensive Mesh Phase Liquid Crystal in Aqueous Mixtures of a Long Chain Nonionic Surfactant, *J. Phys. Chem.*, 1995, **99**, 6054–6063.

61 K. L. Huang, K. Shigeta and H. Kunieda, in *Trends in Colloid and Interface Science XII*, eds. G. J. M. Koper, D. Bedeaux, C. Cavaco and W. F. C. Sager, Progress in Colloid & Polymer Science, vol. 110, 1998, pp. 171–174.

62 M. C. Holmes, Intermediate phases of surfactant-water mixtures, *Curr. Opin. Colloid Interface Sci.*, 1998, **3**, 485–492.

63 S. Dutt, P. F. Siril and S. Remita, Swollen liquid crystals (SLCs): a versatile template for the synthesis of nano structured materials, *RSC Adv.*, 2017, **7**, 5733–5750.

64 W. L. Hinze, *Cloud Point Extraction and Preconcentration Procedures for Organic and Related Pollutants of State Concern*, Water Resources Research Institute of the University of North Carolina, 1992.

65 P. Levitz, Aggregative adsorption of nonionic surfactants onto hydrophilic solid/water interface. Relation with bulk micellization, *Langmuir*, 1991, **7**, 1595–1608.

66 J. M. Corkill, J. F. Goodman and R. H. Ottewill, Micellization of homogeneous non-ionic detergents, *Trans. Faraday Soc.*, 1961, **57**, 1627–1636.

67 C.-C. Chen, Molecular thermodynamic model for gibbs energy of mixing of nonionic surfactant solutions, *AIChE J.*, 1996, **42**, 3231–3240.

68 K.-V. Schubert, R. Strey and M. Kahlweit, A new purification technique for alkyl polyglycol ethers and miscibility gaps for water-CiEj, *J. Colloid Interface Sci.*, 1991, **141**, 21–29.

69 J. M. Corkill, J. F. Goodman and R. H. Ottewill, Micellization of homogeneous non-ionic detergents, *Trans. Faraday Soc.*, 1961, **57**, 1627–1636.

70 J. S. Marland and B. A. Mulley, Effect of micelle formation and the nature of the oil-phase on the distribution of a non-ionic surfactant in three- and four-component emulsions, *J. Pharm. Pharmacol.*, 1972, **24**, 729–734.

71 P. Levitz, Aggregative adsorption of nonionic surfactants onto hydrophilic solid/water interface. Relation with bulk micellization, *Langmuir*, 1991, **7**, 1595–1608.

View Article Online
DOI: 10.1039/D1SM00362C

72 F. Portet, P. L. Desbene and C. Treiner, Adsorption Isotherms at a Silica/Water Interface of the Oligomers of Polydispersed Nonionic Surfactants of the Alkylpolyoxyethylated Series., *J. Colloid Interface Sci.*, 1997, **194**, 379–391.

73 C.-C. Chen, Molecular thermodynamic model for gibbs energy of mixing of nonionic surfactant solutions, *AIChE J.*, 1996, **42**, 3231–3240.

74 A. Gezae Daful, V. A. Baulin, J. Bonet Avalos and A. D. Mackie, Accurate Critical Micelle Concentrations from a Microscopic Surfactant Model, *J. Phys. Chem. B*, 2011, **115**, 3434–3443.

75 F. Yuan and R. G. Larson, Multiscale Molecular Dynamics Simulations of Model Hydrophobically Modified Ethylene Oxide Urethane Micelles, *J. Phys. Chem. B*, 2015, **119**, 12540–12551.

76 S. Puvvada and D. Blankschtein, Molecular-thermodynamic approach to predict micellization, phase behavior and phase separation of micellar solutions. I. Application to nonionic surfactants, *J. Chem. Phys.*, 1990, **92**, 3710–3724.

77 J. S. Marland and B. A. Mulley, Effect of micelle formation and the nature of the oil-phase on the distribution of a non-ionic surfactant in three- and four-component emulsions, *J. Pharm. Pharmacol.*, 1972, **24**, 729–734.

78 S. D. Anogiannakis, P. C. Petris and D. N. Theodorou, Promising Route for the Development of a Computational Framework for Self-Assembly and Phase Behavior Prediction of Ionic Surfactants Using MARTINI, *J. Phys. Chem. B*, 2020, **124**, 556–567.

79 A. P. Santos and A. Z. Panagiotopoulos, Determination of the critical micelle concentration in simulations of surfactant systems, *J. Chem. Phys.*, 2016, **144**, 44709.